ARTICLE

# Encapsulation of 2−3-nm-Sized ZnO Quantum Dots in a $SiO_2$ Matrix and Observation of Negative Photoconductivity

**Shrabani Panigrahi, Ashok Bera, and Durga Basak***

Department of Solid State Physics, Indian Association for the Cultivation of Science, Jadavpur, Kolkata 700032, India

**ABSTRACT** Quantum dots (QDs) of ZnO of 2−4 nm size have been encapsulated within a $SiO_2$ matrix using aqueous chemically grown ZnO nanoparticles in a precursor of tetraethyl orthosilicate. The microstructure shows almost a uniform embedment of the QDs in the $SiO_2$ matrix, resulting in a ZnO QDs−$SiO_2$ composite structure. The photocurrent transients of the composite show an instant fall in the current followed by an exponential decay under ultraviolet (UV) illumination, causing negative photoconductivity (NPC), in contrast to the positive photoconductivity in only ZnO nanoparticles. The interface defect states due to the presence of the $SiO_2$ network around ZnO act as charge trap centers for the photoexcited electrons and are responsible for the NPC. The presence of interface-trapped charges under UV illumination has been further confirmed from capacitance−voltage measurements.

**KEYWORDS:** quantum dots • composite • photoconductivity • ZnO

## INTRODUCTION

The growth and assembly of nanomaterials for new applications are at the forefront of nanoscience and nanotechnology research because of their interesting properties related to the specific structures (1, 2). The optical and electronic properties of Si or Ge nanocrystals embedded in an insulator have attracted a great deal of attraction because of their potential applications in memory and optoelectronic devices (3−6). Recently, the silica-based nanocomposites are considered the most challenging systems for the quantum confinement of semiconductive nanocrystallites for better control of the shape, size, and properties (7). Because ZnO has potential uses in efficient UV detection and photonics (8−10), a ZnO−$SiO_2$ nanocomposite system is considered an important assembly for the UV optoelectronic applications. Quite a few attempts have been reported to fabricate a ZnO−$SiO_2$ composite (11−14), where sol−gel and sputtering techniques have been used to produce either ZnO clusters or nonuniformly distributed ZnO nanoparticles (with a wide size distribution of 5−16 or 5−35 nm) in $SiO_2$. The reports mostly have presented interesting structural, morphological, and optical properties owing to the embedment of the nanocrystals within the insulating matrix, but no studies on the photoconductivity properties of such a composite are available in the literature. However, it would be interesting to investigate the photoconducting properties (which largely depends on the size and interface) of such a nanocomposite. Therefore, in this paper, we report on the encapsulation of ZnO quantum dots (QDs) with a uniform size of 2−3 nm in a $SiO_2$ matrix and their UV photoresponse properties. We have observed an interesting phenomenon of negative photoconductivity (NPC), i.e., a decrease in the photocurrent under steady UV illumination, which is not only an important finding but also a novel one for ZnO QDs−$SiO_2$ composites. We have investigated and correlated the NPC with the interface states of ZnO.

## EXPERIMENTAL SECTION

ZnO−$SiO_2$ nanocomposites were prepared in two steps. At first, ZnO nanoparticles were prepared. For this, zinc acetate-2-hydrate [$Zn(CH_3COOH)_2 \cdot 2H_2O$; Sigma-Aldrich, 99.999%] and hexamethylenetetramine [HMT; $(CH_2)_6N_4$, Merck, 99.5%] were mixed thoroughly in deionized water for 1 h under constant stirring by keeping the concentration of $Zn(CH_3COO)_2 \cdot 2H_2O$ and HMT as 10 mM, and the resulting mixture was heated in a beaker at 90 °C. Nanocrystals grew after 2 h and precipitated at the bottom of the beaker. The precipitate was then isolated by centrifugation, washed with ethanol and water several times, and dried under vacuum. As-prepared ZnO nanoparticles were added to a solution containing 20 mL of ethanol, 9 mL of distilled water, and 0.5 mL of $NH_3 \cdot H_2O$ (25 wt %). Then, 0.5 mL of the precursor tetraethyl orthosilicate was added to the mixture dropwise. The solution was kept under constant ultrasonic stirring for about 1 h. After 3 h, the precipitate was isolated and washed with ethanol and water. Finally, the powder was dried under a vacuum. The powder was then heat treated at 600 °C for better crystallization of ZnO.

Structural analysis of the ZnO−$SiO_2$ powder was done using a X-ray diffractometer with Cu Kα radiation ($\lambda = 1.5406$ nm). The surface morphology was examined by high-resolution transmission electron microscopy [HRTEM; model JEOL JSM-2010]. Energy-dispersive X-ray spectroscopy (EDS) was done using a field-emission scanning electron microscope (JEOL JSM-6700F). For photoconductivity measurements, pellets with a diameter of 8 mm were made by a pelletizer using annealed ZnO and ZnO−$SiO_2$ powders. For the purpose of direct-current (dc) measurements, the gold metal electrodes (of 1 mm diameter) were deposited in a circular form on the surface of the

* To whom correspondence should be addressed. E-mail: sspdb@iacs.res.in. Fax: (91) (33) 24732805.
Received for review August 17, 2009 and accepted September 22, 2009

DOI: 10.1021/am9005513



Published on Web 10/01/2009

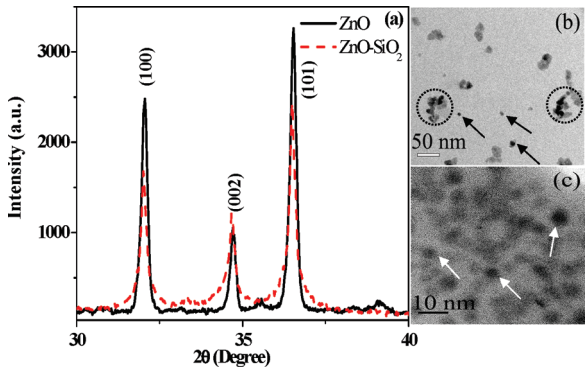


**FIGURE 1. (a) XRD pattern of the as-grown bare ZnO nanoparticles and ZnO−$SiO_2$ composite powder. There is no peak for the amorphous phase of $SiO_2$. (b and c) TEM micrographs of the as-grown bare ZnO nanoparticles and ZnO−$SiO_2$ composite. The marked circles show the agglomeration. The arrows show the single nanoparticle size.**

pellets using a thermal evaporator. The dark current−voltage (*I*−*V*) measurements were done by keeping the sample in the dark and measuring the dc between the two contacts using a Keithley source meter (model 2400) when biased at a certain voltage. All measurements were performed at room temperature.

## RESULT AND DISCUSSION

The X-ray diffraction (XRD) patterns of the as-grown ZnO nanoparticles and ZnO−$SiO_2$ nanocomposite are compared in Figure 1. It shows that both the samples have a hexagonal wurtzite structure without the presence of any impurity. However, in the composite, the peaks have been broadened compared to the bare ZnO. The TEM images show the morphology of the ZnO particles in bare and composite structures. The agglomeration of the bare ZnO nanoparticles is obvious (marked by the dotted circles). It may be observed that the ZnO particles are dispersed in the $SiO_2$ matrix almost uniformly, and the agglomeration is much less. The sizes of the as-grown nanoparticles are calculated to be ∼13 and ∼7 nm (marked with the arrows) for the bare and composite structures, respectively. The decrease in the size of the ZnO crystals in the composite structure is reflected in the broadening of the XRD peaks, which can be attributed to the surface stress in the encapsulated nanoparticles. Figure 2a shows the X-ray diffractogram of the heated nanocomposite, where the peaks corresponding to the hexagonal wurtzite structure of ZnO are sharper compared to those of the as-grown nanoparticles, indicating better crystalline quality (15). Being amorphous, $SiO_2$ does not show any crystalline peak. The pattern further indicates the phase purity of ZnO in the amorphous matrix. The microstructure of the ZnO−$SiO_2$ nanocomposite powder is revealed in the TEM as shown in Figure 2b. The morphology of the composite powder in Figure 2c,d clearly shows the dispersion of the spherical nanocrystals in the matrix of $SiO_2$. The diameter of the nanocrystals is in the range 2−3 nm. The exciton Bohr radius of ZnO has been reported at various sizes, but all report a radius of less than 2.5 nm (16, 17). Therefore, the size of ZnO in this study is comparable to the Bohr radius, and thus these particles can be termed as QDs. The size of the ZnO nanoparticles is reduced upon heating,

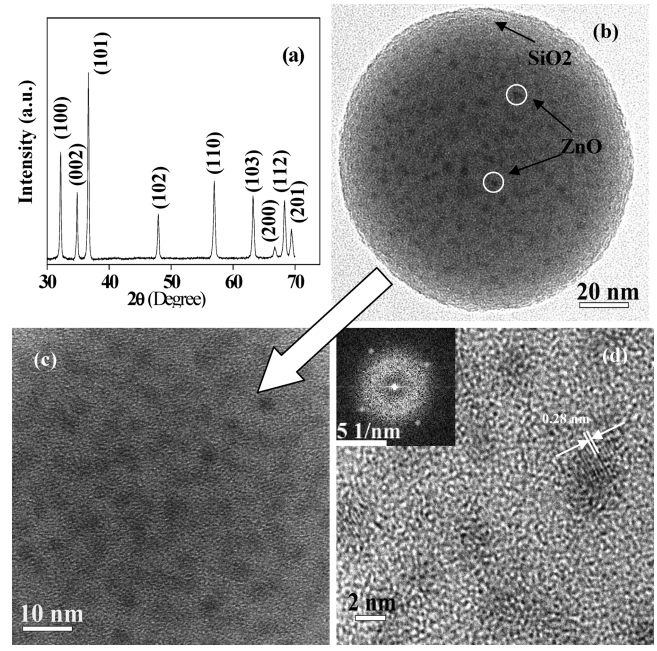


**FIGURE 2. (a) XRD pattern of the ZnO QDs−$SiO_2$ composite powder. There is no peak for the amorphous phase of $SiO_2$. (b and c) TEM micrographs of the ZnO QDs−$SiO_2$ composite in two different magnifications. (d) HRTEM image showing lattice fringes of the corresponding (100) plane of the wurtzite structure. The inset shows the FFT pattern of the standard hexagonal structure of ZnO.**

which was observed earlier in the case of gold nanoparticles (18). The interface between ZnO and $SiO_2$ is prominently visible. The HRTEM image in Figure 2d shows the lattice fringes corresponding to the (100) plane of the ZnO wurtzite structure. The inset shows the corresponding fast Fourier transform (FFT) pattern of ZnO QDs, which is identical with the standard indexed diffraction pattern for the hexagonal crystal structure. Using a modified Spanhel and Anderson method (19), Li et al. (20) have formed QDs of similar size, which reveals an irregular distribution of the QDs in the insulating $SiO_2$ matrix. Our results show that when using such a simple two-step method, a ZnO QDs−$SiO_2$ composite can be synthesized where no agglomeration of the QDs occurs during storage, which is very important for their practical application. The EDS spectrum in Figure S1 of the Supporting Information shows the presence of Zn, Si, and O. The weight percentages of ZnO and $SiO_2$ are calculated to be 39% and 61%, respectively.

The dark and photo-*I*−*V* characteristics of the composite are shown in Figure 3. It shows that the current increases linearly with an increase in the voltage and is symmetrical in both the forward and reverse bias directions, which indicates that the contacts are ohmic. It shows a maximum current value of $8.17 \times 10^{-7}$ A at 10 V. An interesting change is noted when the UV illumination is focused on the sample. At all voltage values, the current value is lower than that in the dark conditions, indicating a negative photoresponse to the UV light. Thus, the photocurrent transients were measured to investigate the temporal response of the photocurrent under steady illumination (Figure 4a). It shows that, at 20 V bias conditions, the dark value is $1.5 \times 10^{-6}$ A, which

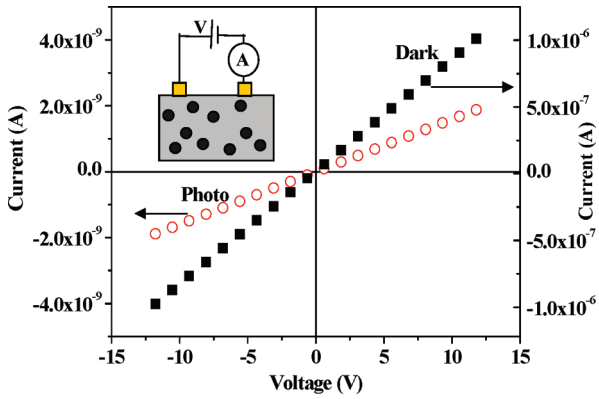


FIGURE 3. dc $I-V$ characteristics of the ZnO QDs−$SiO_2$ composite powder under UV light and dark conditions. The inset shows the experimental setup for the measurement of $I-V$ characteristics through two lateral gold contacts on the pellet.

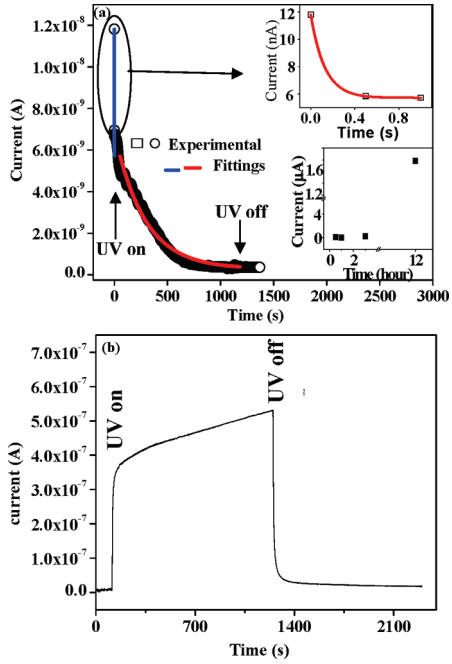


FIGURE 4. Photocurrent transient for the (a) ZnO QDs−$SiO_2$ composite and (b) only ZnO. Blue and red lines represent the corresponding theoretical fittings of the experimental curve. The upper inset shows the magnified graph of the initial instant fall of the photocurrent with time and the corresponding theoretical fittings. The lower inset shows an increase in the current with time after switching of the light.

is the equilibrium value achieved by keeping the sample in the dark for a day or so.

As soon as the UV light is switched on, the current falls instantly and then exponentially to a value of $5.243 \times 10^{-10}$ A in about 20 min. The decrease in the current is by 2 orders of magnitude. In order to confirm that the NPC is truly occurring in the nanocomposite, we measured the photoconductivity of bare ZnO nanoparticles, as shown in Figure 4b. The photocurrent transients in the figure show positive UV response; i.e., the photocurrent increases by 50 times when UV light falls on the sample. Therefore, it confirms that the observed NPC occurs as a result of encapsulation of ZnO in $SiO_2$. Because the dark-to-photocurrent ratio is about $1 \times 10^3$ at 20 V, this composite material can be used to detect the UV radiation in the photodetector and optical switches.

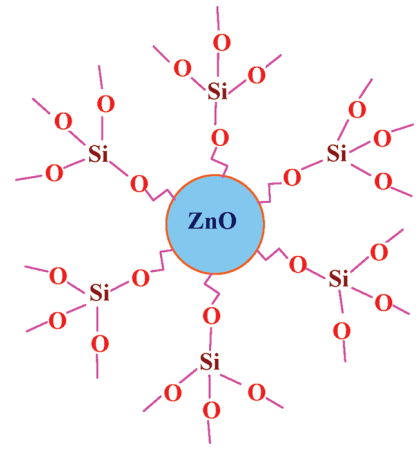


FIGURE 5. Model showing the surface interaction of ZnO with long-chain $SiO_2$ molecules.

Although the NPC was already observed earlier in $In_{0.52}Al_{0.48}As/In_{0.7}Ga_{0.3}As$ heterostructures (21), silicon doped with gold (22), silicon embedded in a $SiO_2$ matrix (23), germanium nanocrystals embedded in $HfO_2$ (24), CdSe embedded in $SiO_2$ (25), and $(ZnO)_x(CdO)_{1-x}$ films (26), the similar phenomenon in ZnO embedded in a $SiO_2$ matrix as observed in our study has not been reported yet. The following explanation can be elucidated to account for the NPC. In the case of ZnO nanocrystals, $O_2$ molecules are chemisorbed and physisorbed onto the crystal surfaces and get ionized as $O_2^-$ by trapping electrons from the bulk. The photons with energy above the band gap are absorbed by ZnO, generating electron−hole pairs. These photoexcited holes are trapped by the adsorbed $O_2^-$ through the surface electron−hole recombination, while the photoexcited unpaired electrons significantly increase the conductivity due to the increased lifetime (27−29). In general, this is the reason behind the large positive UV photoresponse of ZnO. However, in a ZnO−$SiO_2$ nanocomposite, the interface properties of ZnO are quite different because of the presence of a long-chain $SiO_2$ network around the QDs. The interaction of the ZnO surface with $SiO_2$ is shown through a model in Figure 5. When the UV illumination is on, the photoexcited electron−hole pair is generated. These hot electrons are trapped at the interface trap centers, while the holes are trapped at the recombination centers in ZnO. We speculate that the recombination of the free electrons with the trapped hole leads to a reduction in the number of carriers in ZnO and thus results in the NPC. As soon as the UV light is on, initially the photocurrent drops very fast, followed by a relatively slower exponential decay. The initial very fast decay was fitted separately, following the equation $I = I_0 e^{-t/\tau}$, which gave a time constant of 0.128 s (the inset in Figure 4). The rest of the curve was fitted entirely with an exponential equation of the above type, and the time constant in this case was found to be 282 s. Therefore, it is clear that there are two processes responsible for the decay in the photocurrent: one a trapping process (faster time constant) and the second a recombination process (slower time constant). The value of the current increases after the light is switched off. This increase is too slow, so that almost after 12 h, it regains its

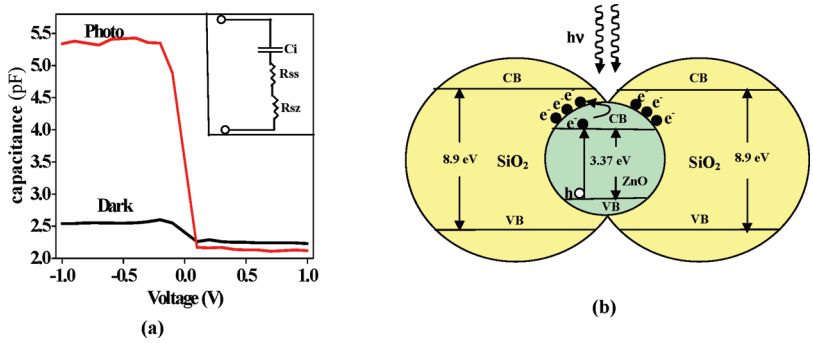


**FIGURE 6. (a) $C-V$ plot of the ZnO QDs−$SiO_2$ composite sample under light and dark conditions. The inset shows the equivalent circuit diagram, where $C_i$ represents the interface capacitance and Rss and Rsz represent the resistances of $SiO_2$ and ZnO. (b) Schematic model for the band diagram of the ZnO QDs−$SiO_2$ composite showing the trapping of the charge carriers at the interface states under UV illumination.**

original dark current value. The increase in the current is due to the slow detrapping of the carriers from the defects.

The trapping of the charge carriers at the interface states was further confirmed by $C-V$ measurements (Figure 6a). The $C-V$ plot at 2 MHz frequency shows that, compared to the dark conditions, the capacitance value under the UV illumination condition is higher, indicating a higher interface trapped charge density when UV light is absorbed. The energy band diagram of the composite and trapping of the carriers by the interface defect states under illumination may be modeled as shown in Figure 6b.

## CONCLUSION

In summary, we have encapsulated 2−4-nm-sized ZnO QDs in a $SiO_2$ matrix. The UV photoresponse properties of the ZnO−$SiO_2$ nanocomposite have been investigated, and the NPC has been observed. The photocurrent transient shows an exponential fall in the current under steady UV illumination. We speculate that the NPC originates from the trapping of the photoexcited hot electrons by the trap centers at the interface defect states due to the presence of a $SiO_2$ network around the 2−3 nm QDs, which is further supported by the higher capacitance value under illuminated conditions. The encapsulation of 2−3-nm-sized QDs in an insulating matrix and the observation of the NPC phenomenon in a composite system are the novel results that can be utilized for UV photodetection and optical switches.

**Acknowledgment.** The authors S.P. and A.B. thank the Council of Scientific and Industrial Research, India, for financial support in the form of a research fellowship. The authors acknowledge the HRTEM facility created by the Department of Science and Technology, New Delhi, India.

**Supporting Information Available:** EDS spectrum (Figure S1). This material is available free of charge via the Internet at http://pubs.acs.org.

## REFERENCES AND NOTES

(1) Qin, Y.; Wang, Z. L. *Nano Lett.* **2009**, *9*, 1103.
(2) Ozin, G. A. *Adv. Mater.* **1992**, *4*, 612.
(3) Baron, T.; Frnandese, A.; Damlencourt, J. F.; De Salvo, B.; Martin, F.; Mazen, F.; Haukka, S. *J. Appl. Phys.* **2003**, *82*, 4151.
(4) Wan, Q.; Zhang, N. L.; Liu, W. L.; Lin, C. L.; Wang, T. H. *Appl. Phys. Lett.* **2003**, *83*, 138.
(5) Wilkinson, A. R.; Elliman, R. G. *J. Appl. Phys.* **2004**, *96*, 4018.
(6) Sias, U. S.; Moreira, E. C.; Ribeiro, E.; Boudinov, H.; Amaral, L.; Behar, M. *J. Appl. Phys.* **2004**, *95*, 5053.
(7) Charkrabarti, S.; Das, D.; Ganguli, D.; Chaudhuri, S. *Thin Solid Films.* **2003**, *441*, 228.
(8) Kind, H.; Yan, H.; Messer, B.; Law, M.; Yang, P. *Adv. Mater.* **2002**, *14*, 158.
(9) Jin, Y.; Wang, J.; Sun, B.; Blakesley, J. C.; Greenham, N. C. *Nano Lett.* **2008**, *8*, 1649.
(10) Lee, J.; Yoon, M. *J. Phys. Chem. C* **2009**, *113*, 11952.
(11) Zhang, W. H.; Shi, J. L.; Wang, L. Z.; Yan, D. S. *Chem. Mater.* **2000**, *12*, 1408.
(12) Mayer, G.; Fonin, M.; Rudiger, U.; Schneider, R.; Gerthsen, D.; Janssen, N.; Bratschitsch, R. *Nanotechnology* **2009**, *20*, 075601.
(13) Burova, L. I.; Petukhov, D. I.; Eliseev, A. A.; Lukashin, A. V.; Tretyakov, Yu. D. *Superlattices Microstruct.* **2006**, *39*, 257.
(14) Musat, V.; Fortunato, E.; Petrescu1, S.; Botelho do Rego, A. M. *Phys. Status Solidi A* **2008**, *205*, 2075.
(15) Li, F.; Huang, X.; Jiang, Y.; Liu, L.; Li, Z. *Mater. Res. Bull.* **2009**, *44*, 437.
(16) Senger, R. T.; Bajaj, K. K. *Phys. Rev. B* **2003**, *68*, 045313.
(17) Sun, Z.; Zhao, B.; Lombardi, J. R. *Appl. Phys. Lett.* **2007**, *91*, 221106.
(18) Li, W.-H.; Wu, S. Y.; Yang, C. C.; Lai, S. K.; Lee, K. C.; Huang, H. L.; Yang, H. D. *Phys. Rev. Lett.* **2002**, *89*, 135504.
(19) Chen, H. G.; Shi, J. L.; Chen, H. R.; Yan, J. N.; Li, Y. S.; Hua, Z. L.; Yang, Y.; Yan, D. S. *Opt. Mater.* **2004**, *25*, 79.
(20) Li, Y. Q.; Yang, Y.; Sun, C. Q.; Fu, S. Y. *J. Phys. Chem. C* **2008**, *112*, 17397.
(21) Akazakia, T.; Yamaguchia, M.; Tsumurac, K.; Nomuraa, S.; Takayanagi, H. *Physica E* **2008**, *40*, 1341.
(22) Kimura, H.; Kurosu, T.; Akiba, Y.; Iida, M. *Appl. Phys. A: Mater. Sci. Process.* **1991**, *53*, 194.
(23) Choi, S. H.; Elliman, R. G. *Appl. Phys. Lett.* **1999**, *74*, 3987.
(24) Wang, S.; Liu, W.; Zhang, M.; Song, Z.; Lin, C.; Dai, J. Y.; Lee, P. F.; Chan, H. L.; Choy, W. C. L. *J. Nanosci. Nanotechnol.* **2006**, *6*, 205.
(25) Kafadaryan, E. A.; Levichev, S.; Pinto, S. R. C.; Aghamalyan1, N. R.; Hovsepyan1, R. K.; Badalyan, G. R.; Chahboun, A.; Rolo, A. G.; Gomes, M. J. M. *Semicond. Sci. Technol.* **2008**, *23*, 095025.
(26) Kavasoglu, N.; Kavasoglu, A. S.; Oktik, S. *J. Phys. Chem. Solids* **2009**, *70*, 521.
(27) Soci, C.; Zhang, A.; Xiang, B.; Dayeh, S. A.; Aplin, D. P. R.; Park, J.; Bao, X. Y.; Lo, Y. H.; Wang, D. *Nano Lett.* **2007**, *7*, 1003.
(28) Bera, A.; Basak, D. *Appl. Phys. Lett.* **2008**, *93*, 053102.
(29) Bera, A.; Basak, D. *ACS Appl. Mater. Interfaces* **2009**, DOI: 10.1021/am900422y.

AM9005513